Efficient and rapid accuracy estimation of the Earth's gravitational field from next-generation GOCE Follow-On by the analytical method*

Zheng Wei(郑 伟)[a)†], Hsu Hou-Tse(许厚泽)[a)], Zhong Min(钟 敏)[a)], Liu Cheng-Shu(刘成恕)[a)], and Yun Mei-Juan(员美娟)[b)]

[a)] *State Key Laboratory of Geodesy and Earth's Dynamics, Institute of Geodesy and Geophysics, Chinese Academy of Sciences, Wuhan* 430077, *China*
[b)] *Department of Applied Physics, Wuhan University of Science and Technology, Wuhan* 430081, *China*

(Received 13 June 2012; revised manuscript received 1 November 2012)

Firstly, a new analytical error model of the cumulative geoid height using the three-dimensional diagonal tensors of satellite gravity gradiometry (SGG) is introduced based on the variance-covariance matrix principle. Secondly, a study for the requirements demonstration on the next-generation GOCE Follow-On satellite gravity gradiometry system is developed using different satellite orbital altitudes and measurement accuracies of satellite gravity gradiometer by the new analytical error model of SGG. The research results show that it is preferable to design satellite orbital altitudes of 300 km–400 km and choose the measurement accuracies of 10^{-13}/s^2–10^{-15}/s^2 from satellite gravity gradiometer. Finally, the complementarity of the four-stage satellite gravity missions, including past CHAMP, current GRACE, and GOCE, and next-generation GOCE Follow-On, is contrastively demonstrated for precisely recovering the Earth's full-frequency gravitational field with high spatial resolution.

Keywords: GOCE Follow-On satellite, analytical method, requirements demonstration, satellite gravity gradiometry, Earth's gravitational field

PACS: 91.10.−v **DOI:** 10.1088/1674-1056/22/4/049101

1. Introduction

Since the Italian physicist Galileo first surveyed gravity at the end of the 16th century, many scholars have carried out extensive gravity studies.[1–7] Different from precisely measuring the Earth's medium-low-frequency gravitational field from the twin gravity recovery and climate experiment (GRACE) satellites, the European Space Agency (ESA) successfully launched the dedicated gravity gradiometry satellite from the gravity field and steady-state ocean circulation explorer (GOCE) in 2009 for accurately determining the Earth's medium-high-frequency gravitational field. The GOCE satellite was injected into an almost circular orbit with an eccentricity of 0.001, a near polar orbit with an inclination of 96.5° and a sun-synchronous orbit at a mean orbital altitude of 250 km during a lifetime of at least 3 years. In the satellite-to-satellite in the high/low tracking (SST-HL) mode associated with the SGG from the GOCE system, except for the precise orbit determination of the low-orbit GOCE satellite with an accuracy of 1 cm by the high-orbit global positioning system (GPS) and global navigation satellite system (GLONASS), the second-order gradients of the Earth's geopotential field at the satellite orbit are precisely determined by the spaceborne electrostatically suspended gradiometer, located at the satellite's center-of-mass (COM), with a measurement accuracy of 3×10^{-12}/s^2.[8] GOCE achieves a drag-free perfection: firstly, the linear acceleration of the satellite's COM and the angular acceleration of the satellite flatform resulted in the non-conservative forces are measured using the spaceborne gradiometer; secondly, the non-conservative forces, including atmospheric drag, solar radiation pressure, Earth's albedo, orbit altitude, and attitude control forces, etc., are accurately compensated by the drag-free attitude control system (DFACS). Therefore, the accuracy of recovering the Earth's gravitational field may be highly improved by accurately and real-timely deducting the non-conservative forces acting on the GOCE satellite. Due to the outstanding contributions to precisely mapping the Earth's medium-high-frequency gravitational field from GOCE and the end of SGG mission before 2015, many scientific institutions in the interdisciplinary field are carrying out the research demonstrations on the next-generation GOCE Follow-On mission for further improving the accuracy of the Earth's gravitational field and precisely obtaining the time-variable gravity signals.[9–13]

*Project supported by the Main Direction Program of Knowledge Innovation of Chinese Academy of Sciences for Distinguished Young Scholar (Grant No. KZCX2-EW-QN114), the National Natural Science Foundation of China for Young Scholar (Grant Nos. 41004006, 41131067, 11173049, and 41202094), the Merit-based Scientific Research Foundation of the State Ministry of Human Resources and Social Security of China for Returned Overseas Chinese Scholars (Grant No. 2011), the Open Research Fund Program of the Key Laboratory of Computational Geodynamics of Chinese Academy of Sciences (Grant No. 2011-04), the Open Research Fund Program of the Key Laboratory of Geospace Environment and Geodesy, Ministry of Education, China (Grant No. 11-01-02), the Open Research Fund Program of the Key Laboratory of Geo-Informatics of National Administration of Surveying, Mapping and Geoinformation of China (Grant No. 201322), the Open Fund of State Key Laboratory of Oil and Gas Reservoir Geology and Exploitation (Grant No. PLN1113), and the Foundation of State Key Laboratory of Petroleum Resources and Prospecting, China University of Petroleum, Beijing (Grant No. PRP/open-1206).

†Corresponding author. E-mail: wzheng@asch.whigg.ac.cn

© 2013 Chinese Physical Society and IOP Publishing Ltd

In the various types of the existing approaches for satellite gravity recovery, the numerical and analytical methods are classified by the differences of establishing and solving the observation equations of the satellite. The numerical method[14–17] is that the observation equation of the satellite is established by analyzing the relationship between the Earth's geopotential coefficients and satellite observations, and the geopotential coefficients are solved using the least-squares principle. The advantage of the numerical method is that the accuracy of the Earth's gravitational field recovery can be greatly improved, and the disadvantages are the slow computational speed and the high requirements for computer performance. We recovered the Earth's gravitational field from GOCE complete up to degree and order 250 based on the time-space-wise numerical approach associated with the Kaula regularization for studying the influences of SGG on the accuracy of the Earth's medium-high-frequency gravitational field in 2011.[17] The analytical method represents that the accuracy of the Earth's gravitational field is estimated based on the error models created by the relationship between the cumulative geoid height errors and the error sources of the gravity satellite system. The advantages of the analytic method are the well-defined physical significance, the facile error analysis and the low computational complexity. The disadvantage is the approximate calculations in the process of establishing error models of the cumulative geoid height. Owing to the high complexity of satellite gravity recovery, it is extremely difficult to accurately set up the analytical error model of cumulative geoid height for describing the whole processes of determining the Earth's gravitational field. However, during the stage of the requirements analysis for the Earth's gravitational field recovery before launching gravity satellites, the feasibility and optimum design of the satellite tracking modes, the satellite orbital parameters (e.g., orbital altitude, orbital inclination, and orbital eccentricity), the measurement accuracies of key payloads (e.g., gradiometer, GPS receiver, drag-free attitude control system, accelerometer, and star camera assembly), and the influences of different types of error sources on the accuracy of the Earth's gravitational field recovery may be efficiently and rapidly demonstrated by the analytical method.

We established a new analytical error model of SGG, carried out the requirements analysis of the next-generation GOCE Follow-On system, and demonstrated the complementarity of the four gravity satellites. This study aims to provide the theoretical basis and computational guarantee for the optimal design of the next-generation SGG system.

2. New analytical method

The spherical harmonic series expansion of the geopotential in the Earth-fixed coordinate (EFC) frame can be defined as

$$V(r,\theta,\lambda)=\frac{GM}{R_{\rm e}}\sum_{l=0}^{L}\sum_{m=0}^{l}\left(\frac{R_{\rm e}}{r}\right)^{l+1}\bar{\rm Y}_{lm}(\theta,\lambda)\bar{X}_{lm}, \tag{1}$$

where

$$\bar{\rm Y}_{lm}(\theta,\lambda)=\bar{\rm P}_{l|m|}(\cos\theta)Q_m(\lambda),$$
$$Q_m(\lambda)=\begin{cases}\cos m\lambda, & m\geq 0,\\ \sin|m|\lambda, & m<0,\end{cases}$$

GM is the product of the Earth's mass M and the gravitational constant G, $R_{\rm e}$ represents the mean radius of the Earth, L shows the maximal degree of the spherical harmonic expansion, $r=\sqrt{x^2+y^2+z^2}$ indicates the geocentric radius of the satellite, x, y, z are the three scalar components of position vector $\boldsymbol{r}$, θ, and λ represent the geocentric colatitude and longitude, respectively, $\bar{\rm P}_{lm}(\cos\theta)$ denotes the normalized associated Legendre polynomials of degree l and order m, and $\bar{X}_{lm}=(\bar{C}_{lm},\bar{S}_{lm})$ are the estimated normalized geopotential coefficients.

The second-order gradients of $V(r,\theta,\lambda)$ with respect to x,y,z yields

$$\boldsymbol{\Gamma}=\begin{bmatrix}V_{xx} & V_{xy} & V_{xz}\\ V_{yx} & V_{yy} & V_{yz}\\ V_{zx} & V_{zy} & V_{zz}\end{bmatrix}, \tag{2}$$

where $\boldsymbol{\Gamma}$ is a symmetrical traceless matrix, $V_{xx}+V_{yy}+V_{zz}=0$, with five independent components of the gravity gradient tensors.

The nine components of the gravity gradient tensors can be represented as

$$\begin{aligned}
V_{xx}(r,\theta,\lambda)&=\frac{1}{r}V_r(r,\theta,\lambda)+\frac{1}{r^2}V_{\theta\theta}(r,\theta,\lambda),\\
V_{yy}(r,\theta,\lambda)&=\frac{1}{r}V_r(r,\theta,\lambda)+\frac{1}{r^2}\cot\theta V_\theta(r,\theta,\lambda)+\frac{1}{r^2\sin^2\theta}V_{\lambda\lambda}(r,\theta,\lambda),\\
V_{zz}(r,\theta,\lambda)&=V_{rr}(r,\theta,\lambda),\\
V_{xy}(r,\theta,\lambda)&=V_{yx}(r,\theta,\lambda)=\frac{1}{r^2\sin\theta}[-\cot\theta V_\lambda(r,\theta,\lambda)+V_{\theta\lambda}(r,\theta,\lambda)],\\
V_{xz}(r,\theta,\lambda)&=V_{zx}(r,\theta,\lambda)=\frac{1}{r^2}V_\theta(r,\theta,\lambda)-\frac{1}{r}V_{r\theta}(r,\theta,\lambda),\\
V_{yz}(r,\theta,\lambda)&=V_{zy}(r,\theta,\lambda)=\frac{1}{r\sin\theta}\left[\frac{1}{r}V_\lambda(r,\theta,\lambda)-V_{r\lambda}(r,\theta,\lambda)\right],
\end{aligned} \tag{3}$$

where the first-order gradient of $V(r,\theta,\lambda)$ with respect to r,θ,λ can be denoted as

$$V_r(r,\theta,\lambda)=-\frac{GM}{R_{\rm e}^2}\sum_{l=0}^{L}(l+1)\left(\frac{R_{\rm e}}{r}\right)^{l+2}\sum_{m=0}^{l}(\bar{C}_{lm}\cos m\lambda+\bar{S}_{lm}\sin m\lambda)\bar{\rm P}_{lm}(\cos\theta),$$

$$V_\theta(r,\theta,\lambda) = -\frac{GM}{R_e}\sum_{l=0}^{L}\left(\frac{R_e}{r}\right)^{l+1}\sum_{m=0}^{l}(\bar{C}_{lm}\cos m\lambda + \bar{S}_{lm}\sin m\lambda)\sin\theta\bar{P}'_{lm}(\cos\theta),$$

$$V_\lambda(r,\theta,\lambda) = \frac{GM}{R_e}\sum_{l=0}^{L}\left(\frac{R_e}{r}\right)^{l+1}\sum_{m=0}^{l} m(-\bar{C}_{lm}\sin m\lambda + \bar{S}_{lm}\cos m\lambda)\bar{P}_{lm}(\cos\theta), \quad (4)$$

the second-order gradients of $V(r,\theta,\lambda)$ with respect to r,θ,λ are expressed as

$$V_{rr}(r,\theta,\lambda) = \frac{GM}{R_e^3}\sum_{l=0}^{L}(l+1)(l+2)\left(\frac{R_e}{r}\right)^{l+3}\sum_{m=0}^{l}(\bar{C}_{lm}\cos m\lambda + \bar{S}_{lm}\sin m\lambda)\bar{P}_{lm}(\cos\theta),$$

$$V_{\theta\theta}(r,\theta,\lambda) = \frac{GM}{R_e}\sum_{l=0}^{L}\left(\frac{R_e}{r}\right)^{l+1}\sum_{m=0}^{l}(\bar{C}_{lm}\cos m\lambda + \bar{S}_{lm}\sin m\lambda)[\sin^2\theta\bar{P}''_{lm}(\cos\theta) - \cos\theta\bar{P}'_{lm}(\cos\theta)],$$

$$V_{\lambda\lambda}(r,\theta,\lambda) = -\frac{GM}{R_e}\sum_{l=0}^{L}\left(\frac{R_e}{r}\right)^{l+1}\sum_{m=0}^{l} m^2(\bar{C}_{lm}\cos m\lambda + \bar{S}_{lm}\sin m\lambda)\bar{P}_{lm}(\cos\theta),$$

$$V_{r\theta}(r,\theta,\lambda) = V_{\theta r}(r,\theta,\lambda) = \frac{GM}{R_e^2}\sum_{l=0}^{L}(l+1)\left(\frac{R_e}{r}\right)^{l+2}\sum_{m=0}^{l}(\bar{C}_{lm}\cos m\lambda + \bar{S}_{lm}\sin m\lambda)\sin\theta\bar{P}'_{lm}(\cos\theta),$$

$$V_{r\lambda}(r,\theta,\lambda) = V_{\lambda r}(r,\theta,\lambda) = \frac{GM}{R_e^2}\sum_{l=0}^{L}(l+1)\left(\frac{R_e}{r}\right)^{l+2}\sum_{m=0}^{l} m(\bar{C}_{lm}\sin m\lambda - \bar{S}_{lm}\cos m\lambda)\bar{P}_{lm}(\cos\theta),$$

$$V_{\theta\lambda}(r,\theta,\lambda) = V_{\lambda\theta}(r,\theta,\lambda) = \frac{GM}{R_e}\sum_{l=0}^{L}\left(\frac{R_e}{r}\right)^{l+1}\sum_{m=0}^{l} m(\bar{C}_{lm}\sin m\lambda - \bar{S}_{lm}\cos m\lambda)\sin\theta\bar{P}'_{lm}(\cos\theta), \quad (5)$$

the zero-order, first-order, and second-order derivatives of the Legendre functions are respectively shown as

$$\bar{P}_{lm}(\cos\theta) = \gamma_m 2^{-l}\sin^m\theta\sum_{k=0}^{[(l-m)/2]}(-1)^k\frac{(2l-2k)!}{k!(l-k)!(l-m-2k)!}(\cos\theta)^{l-m-2k},\ (m\le l),$$

$$\bar{P}'_{lm}(\cos\theta) = \frac{1}{\sin\theta}[(l+1)\cos\theta\bar{P}_{lm}(\cos\theta) - (l-m-1)\bar{P}_{l+1,m}(\cos\theta)],$$

$$\bar{P}''_{lm}(\cos\theta) = -l\bar{P}_{lm}(\cos\theta) + l\cos\theta\bar{P}'_{l-1,m}(\cos\theta) + \frac{l}{4}\cos^2\theta[\bar{P}'_{l-1,m+1}(\cos\theta) - 4\bar{P}'_{l-1,m-1}(\cos\theta)], \quad (6)$$

where

$$\gamma_m = \begin{cases}\sqrt{2(2l+1)\dfrac{(l-|m|)!}{(l+|m|)!}}, & (m\neq 0),\\ \sqrt{2l+1}, & (m=0).\end{cases}$$

The matrix expression of Eq. (3) is defined as

$$y = \boldsymbol{A}\cdot x, \quad (7)$$

where y represents the SGG observations, A shows a design matrix, and x denotes the estimated normalized geopotential coefficients $(\bar{C}_{lm},\bar{S}_{lm})$.

Multiplying both sides of Eq. (7) by $\boldsymbol{A}^{\mathrm{T}}$ yields

$$\boldsymbol{A}^{\mathrm{T}}y = \boldsymbol{A}^{\mathrm{T}}\boldsymbol{A}\cdot x, \quad (8)$$

where $\boldsymbol{A}^{\mathrm{T}}\boldsymbol{A}$ is the normal matrix.

Based on the least-squares adjustment method and the variance-covariance matrix, the main diagonal elements of $(\boldsymbol{A}^{\mathrm{T}}\boldsymbol{A})^{-1}$ are equal to the error variance of the Earth's geopotential coefficients

$$\sigma_l^2(\bar{C}_{lm},\bar{S}_{lm}) = \sigma_0^2\cdot\mathrm{Diag}(\boldsymbol{A}^{\mathrm{T}}\boldsymbol{A})^{-1}, \quad (9)$$

where σ_0 is the measurement accuracy of the spaceborne gradiometer.

By combining Eqs. (3) and (8), based on the orthonormality of the spherical harmonic functions, the diagonal element of normal matrix $(\boldsymbol{A}^{\mathrm{T}}\boldsymbol{A})_{V_{zz}}$ for the vertical gravity gradient V_{zz} is expressed as

$$\mathrm{Diag}(\boldsymbol{A}^{\mathrm{T}}\boldsymbol{A})_{V_{zz}} = \left(\frac{GM}{R_e^3}\right)^2\left(\frac{R_e}{R_e^+H}\right)^{2l+6}(l+1)^2(l+2)^2, \quad (10)$$

where H is the mean orbital altitude of the satellite.

The diagonal elements of normal matrices $(\boldsymbol{A}^{\mathrm{T}}\boldsymbol{A})_{V_{xx}}$ and $(\boldsymbol{A}^{\mathrm{T}}\boldsymbol{A})_{V_{yy}}$ for the horizontal gravity gradients V_{xx} and V_{yy} are represented as

$$\mathrm{Diag}(\boldsymbol{A}^{\mathrm{T}}\boldsymbol{A})_{V_{xx}} \approx \mathrm{Diag}\left(\boldsymbol{A}^{\mathrm{T}}\boldsymbol{A}\right)_{V_{yy}}$$
$$= \left(\frac{GM}{R_e^3}\right)^2\left(\frac{R_e}{R_e+H}\right)^{2l+6}\frac{(l+1)^3(l+2)(2l+3)}{3(2l+1)}. \quad (11)$$

The diagonal elements of normal matrix $(\boldsymbol{A}^{\mathrm{T}}\boldsymbol{A})_{V_{zz}-V_{xx}-V_{yy}}$ for the correlation[18] of V_{xx}, V_{yy}, and V_{zz} are represented as

$$\mathrm{Diag}(\boldsymbol{A}^{\mathrm{T}}\boldsymbol{A})_{V_{zz}-V_{xx}-V_{yy}} = \left(\frac{GM}{R_e^3}\right)^2\left(\frac{R_e}{R_e+H}\right)^{2l+6}$$
$$\times\left[(l+1)(l+2) - 2\sqrt{\frac{(l+1)^3(l+2)(2l+3)}{3(2l+1)}}\right]^2. \quad (12)$$

According to the error theory, if the number of SGG observation points is K_0, the error variance of the Earth's geopo-

tential coefficients is proportional to $1/K_0$

$$K_0 = T/\Delta t, \tag{13}$$

where T is the observation time of the satellite, and Δt is the sampling interval of observation points.

The three diagonal elements (V_{xx}, V_{yy}, V_{zz}) are the main tensors in the nine components of satellite gravity gradients, and the influences of the off-diagonal tensors on the accuracy of the Earth's gravitational field can be basically ignored relative to the diagonal tensors. Therefore, combining Eqs. (9)–(12), the error variance of the Earth's geopotential coefficients for the diagonal tensors V_{ij} of the satellite gravity gradients is denoted as

$$\sigma_l^2(\bar{C}_{lm},\bar{S}_{lm})_{V_{ij}} = \frac{\sigma_0^2}{K_0[\mathrm{Diag}(\boldsymbol{A}^{\mathrm{T}}\boldsymbol{A})_{V_{xx}} + \mathrm{Diag}(\boldsymbol{A}^{\mathrm{T}}\boldsymbol{A})_{V_{yy}} + \mathrm{Diag}(\boldsymbol{A}^{\mathrm{T}}\boldsymbol{A})_{V_{zz}} + \mathrm{Diag}(\boldsymbol{A}^{\mathrm{T}}\boldsymbol{A})_{V_{zz}-V_{xx}-V_{yy}}]}. \tag{14}$$

The error degree variance for the cumulative geoid heights is shown as

$$\sigma_l^2(N) = R_{\mathrm{e}}^2 \sum_{l=0}^{L}\sum_{m=-l}^{l}\left[(\delta\bar{C}_{lm})^2 + (\delta\bar{S}_{lm})^2\right]. \tag{15}$$

where $\delta\bar{C}_{lm}$ and $\delta\bar{S}_{lm}$ represent the errors of the Earth's geopotential coefficients.

By combining Eqs. (10)–(15), the analytical error model of the cumulative geoid height for the vertical tensor V_{zz} of satellite gravity gradients is indicated as

$$\sigma_l(N)_{V_{zz}} = \frac{\sigma_0}{\sqrt{T/\Delta t}}\frac{R_{\mathrm{e}}^4}{GM}\sqrt{\sum_{l=0}^{L}\frac{2l+1}{\left(\frac{R_{\mathrm{e}}}{R_{\mathrm{e}}+H}\right)^{2l+6}(l+1)^2(l+2)^2}}, \tag{16}$$

the analytical error model of cumulative geoid height for the horizontal tensors V_{xx} and V_{yy} of satellite gravity gradients is represented as

$$\sigma_l(N)_{V_{xx}} \approx \sigma_l(N)_{V_{yy}} = \frac{\sigma_0}{\sqrt{T/\Delta t}}\frac{R_{\mathrm{e}}^4}{GM}\sqrt{\sum_{l=0}^{L}\frac{2l+1}{\left(\frac{R_{\mathrm{e}}}{R_{\mathrm{e}}+H}\right)^{2l+6}\frac{(l+1)^3(l+2)(2l+3)}{3(2l+1)}}}, \tag{17}$$

the analytical error model of the cumulative geoid height for the diagonal tensors V_{ij} of satellite gravity gradients is expressed as

$$\sigma_l(N)_{V_{ij}} = \frac{\sigma_0}{\sqrt{T/\Delta t}}\frac{R_{\mathrm{e}}^4}{GM}\sqrt{\sum_{l=0}^{L}\frac{2l+1}{\left(\frac{R_{\mathrm{e}}}{R_{\mathrm{e}}+H}\right)^{2l+6}\left[2(l+1)^2(l+2)^2 + \frac{6(l+1)^3(l+2)(2l+3)}{3(2l+1)} - 4\sqrt{\frac{(l+1)^5(l+2)^3(2l+3)}{3(2l+1)}}\right]}}. \tag{18}$$

3. Requirements demonstration

3.1. Optimum design of orbital altitudes

As has been illustrated in Fig. 1, the solid line represents the accuracy of GOCE Earth gravity field model GO_CONS_GCF_2_DIR_R1[15] complete up to degree and order 240 released by the French Centre National d'Études Spatiales (CNES), and the cumulative geoid height error is 8.523×10^{-2} m at degree 240. The cross, slim dashed, circled, and bold dashed lines respectively express the accuracies of the Earth's gravitational field from the next-generation GOCE Follow-On satellite based on the analytical error model Eq. (17) of cumulative geoid height for the diagonal tensors V_{ij} of satellite gravity gradients using the same measurement accuracy of $10^{-14}/\mathrm{s}^2$ from the spaceborne gradiometer and different orbital altitudes of the satellite between 200 km and 500 km. The statistical results of cumulative geoid height errors from GOCE and GOCE Follow-On based on different orbital altitudes are listed in Table 1, and the related computational parameters of the analytical error model of SGG are displayed in Table 2. The results of this study show that it is preferable to design the orbital altitudes between 300 km and 400 km for the next-generation gravity gradient satellite GOCE Follow-On. The reasons are stated below.

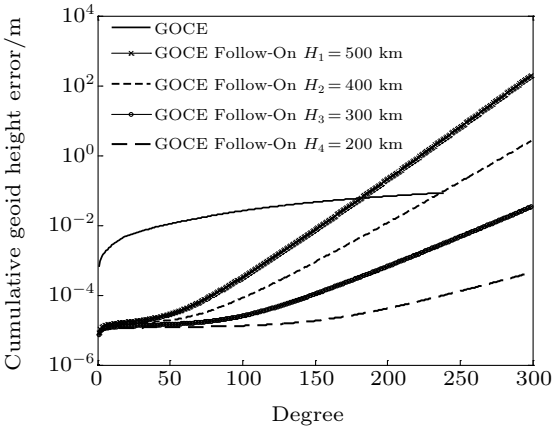


Fig. 1. A comparison of cumulative geoid height errors between GOCE and GOCE Follow-On from different orbital altitudes.

Table 1. Statistical results of cumulative geoid height errors from GOCE and GOCE Follow-On based on different orbital altitudes.

Orbital altitudes/km	Cumulative geoid height errors/m					
	Degree 50	Degree 100	Degree 150	Degree 200	Degree 240	Degree 300
GOCE	1.076×10^{-2}	2.570×10^{-2}	4.571×10^{-2}	6.571×10^{-2}	8.523×10^{-2}	–
$H_1=500$	2.786×10^{-5}	3.075×10^{-4}	7.026×10^{-3}	1.958×10^{-1}	3.028×10^{0}	1.993×10^{2}
$H_2=400$	1.889×10^{-5}	7.975×10^{-5}	8.448×10^{-4}	1.123×10^{-2}	9.648×10^{-2}	2.631×10^{0}
$H_3=300$	1.446×10^{-5}	2.478×10^{-5}	1.043×10^{-4}	6.453×10^{-4}	3.038×10^{-3}	3.379×10^{-2}
$H_4=200$	1.199×10^{-5}	1.319×10^{-5}	1.820×10^{-5}	4.082×10^{-5}	9.954×10^{-5}	4.385×10^{-4}

Table 2. Computational parameters of analytical error model of SGG.

Parameters	Indexes
Orbital altitude H	200 km–500 km
Accuracy of gradiometer σ_0	10^{-12}/s^2–10^{-15}/s^2
Observation time T	60 days
Sampling interval Δt	5 s
Earth's mean radius R_e	6378 km
Gravitational constant GM	3.986004415×10^{14} Nm^2/kg

Firstly, in order to satisfy the requirements of the future gravity satellite for increasing the lifetime of the satellite and acquiring the time-varying signals of the Earth's gravitational field, the orbital altitude of the GOCE Follow-On satellite should be higher than that of the GOCE satellite (200 km–300 km). Additionally, based on the measurement requirements of the next-generation satellite gravity mission that the accuracy of the Earth's gravitational field from GOCE Follow-On is at least one order of magnitude higher than that from GOCE, the orbital altitude of the GOCE Follow-On satellite should be lower than 400 km by a comparison of the solid and slim dashed lines in Fig. 1. As shown in Table 1, the accuracy of the Earth's gravitational field from GOCE is 8.523×10^{-2} m at degree 240, and the accuracy of the Earth's gravitational field from GOCE Follow-On is improved by 28.055 times at an orbital altitude of 300 km compared with GOCE. Therefore, an orbital altitude of 300 km–400 km is preferred to precisely develop the next-generation Earth static and time-variable gravity field model with high spatial resolution according to the recovery requirements of the GOCE Follow-On satellite mission.

Secondly, we know that the GOCE satellite is located at the orbital altitudes of 200 km–300 km derived from the GPS data of GOCE-Level-1B file released by the ESA. The Earth's medium-high-frequency gravitational field with high spatial resolution is accurately mapped by GOCE during an observation time of over 2 years. Because different orbital altitudes of the satellite are sensitive to different frequency-band signals of the Earth's gravitational field, the accuracy of the Earth's gravitational field from GOCE may be only improved in the limited space extent of orbital altitudes. If the orbital altitude of the next-generation gravity gradient satellite is the same as that of GOCE, the repeated measurement will be insignificantly carried out by GOCE Follow-On. Therefore, the unmeasurable area between 300 km and 400 km of the GOCE satellite orbit is an optimum space extent for the orbital altitude of the next-generation gravity gradient satellite in order to make up for the measuring deficiency of the GOCE satellite.

Finally, the critical defect of the gravity satellite to precisely determine the Earth's gravitational field with high spatial resolution is the exponential decay of gravity signals with the increase of orbital altitude of the satellite. In order to solve this problem, a lower orbital altitude of the satellite is an efficient approach to highly improve the accuracy of the Earth's gravitational field. The GOCE satellite is designed to greatly suppress the signal attenuation of the Earth's gravitational field by a low-Earth-orbit (LEO) mode at a mean altitude of 250 km. Although this approach may improve the accuracy of the Earth's gravitational field in theory, the negative impacts on the accuracy of the Earth's gravitational field recovery cannot be ignored in practice. (i) The numerical value of the atmospheric drag will increase by 10 times with the decrease of 100 km on the orbital altitude. The orbital maneuvers have to be frequently performed for real-timely adjusting the orbital altitudes and attitudes of the satellite. Accordingly, an unstable environment of the satellite platform will directly impact on the measurement accuracy of key payloads. (ii) Due to the fuel consumption induced by the frequent jet of the satellite, the real-time offset of the COM between the satellite and the spaceborne gradiometer will affect the measurement accuracy of the spaceborne gradiometer. (iii) The accuracies of the Earth's static and time-varying gravitational field will be reduced by shortening the satellite lifetime. Therefore, the optimum design of orbital altitudes is highly important to precisely recover the Earth's gravitational field with high spatial resolution. For the sake of supplying a gap of the GOCE satellite, the orbital altitude of the next-generation gravity gradient satellite GOCE Follow-On had better be designed in the space extent of 300 km–400 km in order to provide a stable work environment to the satellite platform for key payloads, including the gradiometer, GPS/GLONASS receiver, drag-free attitude system, star camera assembly, etc.

3.2. Optimal choice of measurement accuracy of gradiometer

Figure 2 displays a comparison of cumulative geoid height errors between GOCE (GO_CONS_GCF_2_DIR_R1 model) and the next-generation GOCE Follow-On satellite based on the same orbital altitude of 300 km and different

measurement accuracies of the spaceborne gradiometer between 10^{-12}/s^2 and 10^{-15}/s^2 using the analytical error model Eq. (17) for the diagonal tensors V_{ij} of SGG (Table 1), and the statistical results of cumulative geoid height errors from GOCE and GOCE Follow-On based on different measurement accuracies of the spaceborne gradiometer are listed in Table 3. These results suggest that the measurement accuracies of the spaceborne gradiometer between 10^{-13}/s^2 and 10^{-15}/s^2 are a preferred choice for the next-generation gravity satellite GOCE Follow-On. The reasons are as follows.

Firstly, for the sake of meeting the precision requirements of the future satellite gravity recovery that the development accuracy of the GOCE Follow-On Earth gravity field model is at least improved by 10 times compared with that of GOCE model, the measurement accuracies of the spaceborne gradiometer from the GOCE Follow-On satellite should be higher than 10^{-12}/s^2 by a comparison between the solid and bold dashed lines in Fig. 2. As shown in Table 3, the cumulative geoid height error from GOCE is 8.523×10^{-2} m at degree 240, and cumulative geoid height errors from GOCE Follow-On compared with that from GOCE are improved by 2.808 times, 28.055 times, and 280.546 times based on the measurement accuracies of 10^{-13}/s^2, 10^{-14}/s^2, and 10^{-15}/s^2 from the spaceborne gradiometer, respectively. Therefore, it is preferable for the measurement accuracies of the spaceborne gradiometer to be between 10^{-13}/s^2 and 10^{-15}/s^2 in the next-generation GOCE Follow-On satellite gravity mission.

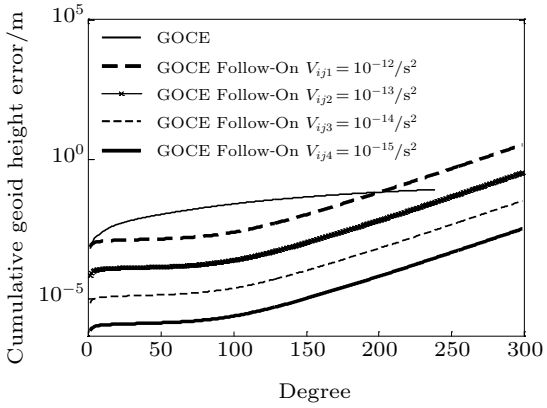


Fig. 2. A comparison of cumulative geoid height errors between GOCE and GOCE Follow-On from different measurement accuracies of the gradiometer.

Table 3. Statistical results of cumulative geoid height errors from GOCE, and GOCE Follow-On based on different measurement accuracies of the gradiometer.

Accuracy/s^{-1}	Cumulative geoid height errors/m					
	Degree 50	Degree 100	Degree 150	Degree 200	Degree 240	Degree 300
GOCE	1.076×10^{-2}	2.570×10^{-2}	4.571×10^{-2}	6.571×10^{-2}	8.523×10^{-2}	–
$V_{ij1} = 10^{-12}$	1.446×10^{-3}	2.478×10^{-3}	1.043×10^{-2}	6.453×10^{-2}	3.038×10^{-1}	3.379×10^{0}
V_{ij2}=10^{-13}	1.446×10^{-4}	2.478×10^{-4}	1.043×10^{-3}	6.453×10^{-3}	3.038×10^{-2}	3.379×10^{-1}
V_{ij3}=10^{-14}	1.446×10^{-5}	2.478×10^{-5}	1.043×10^{-4}	6.453×10^{-4}	3.038×10^{-3}	3.379×10^{-2}
V_{ij4}=10^{-15}	1.446×10^{-6}	2.478×10^{-6}	1.043×10^{-5}	6.453×10^{-5}	3.038×10^{-4}	3.379×10^{-3}

Secondly, the spaceborne gradiometers are classified by different measuring principles including the rotational gravity gradiometer (10^{-8}/s^2–10^{-10}/s^2), electrostatic suspension gravity gradiometer (10^{-10}/s^2–10^{-12}/s^2), the superconducting gravity gradiometer (10^{-10}/s^2–10^{-12}/s^2), the atom-interferometer gravity gradiometer (10^{-13}/s^2–10^{-15}/s^2), etc. A new type of the high-precise atom-interferometer gravity gradiometer is a direction of the mainstream development for the next-generation SGG mission.[19] Therefore, based on the advantages of the high sensitivity, the simple structure, the low cost, and the strong anti-interference ability, the atom-interferometer gravity gradiometer with a measurement accuracy of 10^{-13}/s^2–10^{-15}/s^2 is an optimal choice for the next-generation GOCE Follow-On SGG mission.

3.3. Comparison among four-stage satellite gravity missions

Figure 3 shows a comparison of the accuracies of the Earth's gravitational field recovery from the past CHAMP, the current GRACE, and GOCE, and the future GOCE Follow-On satellite gravity missions, where the cumulative geoid height errors from CHAMP, GRACE, and GOCE are determined using the satellite orbital parameters and the measurement accuracies of key payloads published by the international research institutes including the American Jet Propulsion Laboratory (JPL) and the German GeoForschungsZentrum Potsdam (GFZ). The statistical results of cumulative geoid height errors from CHAMP, GRACE, GOCE, and GOCE Follow-On are listed in Table 4.

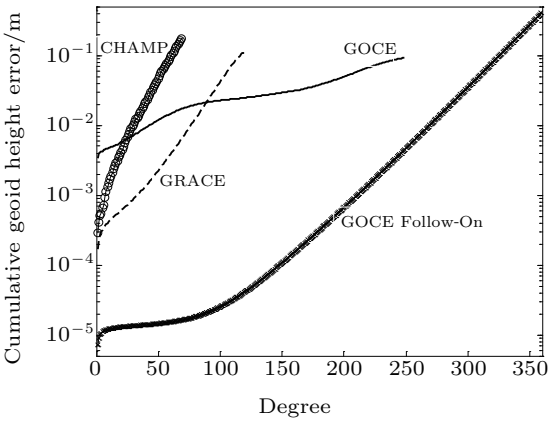


Fig. 3. A comparison of cumulative geoid height errors based on past CHAMP, current GRACE, and GOCE, and next-generation GOCE Follow-On gravity satellites.

Table 4. Statistical results of cumulative geoid height errors from CHAMP, GRACE, GOCE, and GOCE Follow-On.

Gravity satellites	Cumulative geoid height errors/m					
	Degree 20	Degree 50	Degree 70	Degree 120	Degree 250	Degree 360
CHAMP	3.732×10^{-3}	4.226×10^{-2}	1.727×10^{-1}	–	–	–
GRACE	5.851×10^{-4}	2.133×10^{-3}	6.485×10^{-3}	1.098×10^{-1}	–	–
GOCE	5.535×10^{-3}	1.163×10^{-2}	1.718×10^{-2}	2.463×10^{-2}	9.295×10^{-2}	–
GOCE Follow-On	1.289×10^{-5}	1.446×10^{-5}	1.635×10^{-5}	4.036×10^{-5}	4.512×10^{-3}	4.016×10^{-1}

(I) The maximum degree of the spherical harmonic expansion for determining the Earth's gravitational field from CHAMP is about 70 (a spatial resolution of 286 km) based on the SST-HL mode. As shown in Fig. 3, we measured the Earth's gravitational field from CHAMP complete up to degree and order 70 based on the energy conservation principle.[20] The cumulative geoid height error is 17.273 cm at degree 70, which is true of the accuracy of the global gravity field model EIGEN-CHAMP03S[21]released by GFZ. CHAMP is the first dedicated gravity satellite for only measuring the low-frequency signals of the Earth's gravitational field due to the limitations of an orbital altitude of 454 km, a measurement accuracy of key payloads and a satellite tracking mode of SST-HL. The CHAMP mission is an exploratory experiment for recovering the global gravitational field.

(II) The highest degree of the spherical harmonic expansion for mapping the Earth's gravitational field from GRACE is approximately 120 (a spatial resolution of 167 km) based on the satellite-to-satellite tracking in the high-low/low-low model (SST-HL/LL). As displayed in Fig. 3, we developed the GRACE Earth gravity field model WHIGG-GEGM01S complete up to degree and order 120 using the GRACE-Level-1B data products, acquired during 2008-01-01 to 2008-12-31 and released by the JPL based on the Intersatellite Range Interpolation Method (IRIM).[22] The cumulative geoid height error is equal to 10.981 cm at degree 120, which accords with the accuracy of the global gravity field model EIGEN-GRACE02S[23] released by GFZ. In addition, we have developed the extensive research and demonstrations in terms of recovering the Earth's gravitational field from the current GRACE and future GRACE Follow-On missions.[24–43] Our cognitive abilities of the digital-based Earth were enormously improved after the successful launch of the twin GRACE satellite. A new GRACE Earth gravity field model is produced per 15 d–30 d, and the contribution of GRACE to accurately mapping the Earth's gravitational field surpassed the total information content of the past 30 years.

(III) The maximal degree of the spherical harmonic expansion for recovering the Earth's gravitational field from GOCE is approximately 250 (a spatial resolution of 80 km) based on the satellite-to-satellite tracking in the high–low model associated with the SGG mode (SST-HL/SGG). As illustrated in Fig. 3, we recovered the Earth's gravitational field from GOCE complete up to degree and order 250 based on the time-space-wise approach associated with the Kaula regularization, and the cumulative geoid height error is 9.295 cm at degree 250,[17] which tallies with the accuracy of the global gravity field model GO_CONS_GCF_2_DIR_R1[15] released by the French Centre National d'Études Spatiales (CNES). Due to a sharp signal attenuation $(R_e/r)^l$ of the Earth's gravitational field with the increase of the orbital altitude, the analysis of the satellite's orbital motion is only appropriate to determine the Earth's medium-low-frequency gravitational field. However, because the second-order gradients of the Earth's geopotential may be directly measured, SGG may suppress the signal attenuation of the geopotential with the increase of orbital altitude and accurately determine the Earth's medium-high-frequency gravitational field.

(IV) The maximum degree of the spherical harmonic expansion for measuring the Earth's gravitational field from GOCE Follow-On is about 360 (a spatial resolution of 55 km) based on the SST-HL/SGG mode. As illustrated in Fig. 3, we estimated the accuracy of the Earth's gravitational field from GOCE Follow-On up to degree 360 using an orbital altitude of 300 km and a measurement accuracy of $10^{-14}/s^2$ from the spaceborne gradiometer by the new analytical error model in this study, and the other computational parameters are listed in Table 1. The cumulative geoid height error is 40.162 cm at degree 360. The most important reason why the accuracy of the Earth's gravitational field from the next-generation GOCE Follow-On mission is at least one order of magnitude higher than that from the present GOCE mission is that the measurement accuracy of the GOCE Follow-On gradiometer is highly increased by 1–3 orders of magnitude relative to the GOCE gradiometer.

(V) Because the CHAMP, GRACE, GOCE, and GOCE Follow-On gravity satellites respectively aim to detect different frequency-band gravity signals, the high-precision, high-resolution, and full-frequency Earth's gravitational field may be recovered by an efficient combination of the above satellite gravity missions.

4. Conclusion

The most important idea in this study is that a new analytical error model of SGG is established for accurately and rapidly estimating the accuracy of the Earth's gravitational field from GOCE Follow-On.

i) We analyzed the requirements of the next-generation

GOCE Follow-On system based on different orbital altitudes of the satellite and measurement accuracies of the spaceborne gradiometer. Our results suggest the satellite orbital altitudes of 300 km–400 km and the measurement accuracies of 10^{-13}/s^2–10^{-15}/s^2 from the spaceborne gradiometer are the preferred designs for the next-generation GOCE Follow-On satellite.

ii) We demonstrated the complementarity of the four-stage satellite gravity missions. The research findings show that the new global gravitational field model will be precisely produced by a combination of various satellite observation data from CHAMP, GRACE, GOCE, and GOCE Follow-On.

Acknowledgements

We greatly appreciate the helpful and constructive discussion with Prof. Luo J, School of Physics, Huazhong University of Science and Technology, China. The authors would like to thank the European Space Agency (ESA) for providing related information of the GOCE satellite.

References

[1] Zhu Z H, Ge P W, Xu Z Y and Huo C R 1998 *Chin. Phys.* **7** 801
[2] Liu Y C, Chen W C, Huo C R and Ge P W 1999 *Chin. Phys.* **8** 881
[3] Zhu Z H, Ge P W and Xu Z Y 2000 *Chin. Phys.* **9** 321
[4] Chen G 2001 *Chin. Phys.* **10** 787
[5] Wu Y B, Li J L and Li L 2002 *Chin. Phys.* **11** 222
[6] Zhu Z H, Hong Y, Ge P W and Yu Y D 2004 *Chin. Phys.* **13** 1982
[7] Zeng X X, Yang S Z and Chen D Y 2008 *Chin. Phys. B* **17** 1629
[8] Bian S F and Ji B 2006 *Prog. Geophys.* **21** 660
[9] Aguirre-Martinez M and Sneeuw N 2003 *Space Sci. Rev.* **108** 409
[10] Rummel R 2003 *Space Sci. Rev.* **108** 1
[11] Sneeuw N 2005 *Earth, Moon, and Planets* **94** 113
[12] Zheng W, Xu H Z, Zhong M and Yun M J 2012 *Chin. Phys. B* **21** 109101
[13] Klees R, Koop R and Visser P 2000 *J. Geod.* **74** 561
[14] Ditmar P, Klees R and Kostenko F 2003 *J. Geod.* **76** 690
[15] Bruinsma S L, Marty J C, Balmino G, Biancale R, Foerste C, Abrikosov O and Neumayer H 2010 *ESA Living Planet Symposium* 2010, Bergen, Noway, June 27–July 2, 2010, p. 1
[16] Pail R, Goiginger H, Schuh W D, Höck E, Brockmann J M, Fecher T, Gruber T, Mayer-Gürr T, Kusche J, Jäggi A and Rieser D 2010 *Geophys. Res. Lett.* **37** L20314
[17] Zheng W, Xu H Z, Zhong M, Yun M J and Zhou X H 2011 *Chin. J. Geophys.* **54** 240
[18] Liu X G, Wu X P and Wang K 2012 *Chin. J. Geophys.* **55** 1572
[19] Yu N, Kohel J M, Kellogg J R and Maleki L 2006 *Appl. Phys. B: Lasers and Optics* **84** 647
[20] Zheng W, Xu H Z, Zhong M, Yun M J, Zhou X H and Peng B B 2008 *The* 2008 *Annual Meeting Symposium of Chinese Society for Geodesy Photogrammtry and Cartography*, November 5–7, 2008, Guilin, China, p. 372
[21] Reigber Ch 2004 *Earth Observation with CHAMP–Results from Three Years in Orbit*, (Berlin: Springer-Verlag) p. 25
[22] Zheng W, Xu H Z, Zhong M and Yun M J 2012 *J. Geodyn.* **53** 1
[23] Reigber C, Schmidt R, Flechtner F, König R, Meyer U, Neumayer K H, Schwintzer P and Zhu S Y 2004 *J. Geodyn.* **39** 1
[24] Zhang H W and Liu X Q 2004 *Prog. Geophys.* **19** 372
[25] Shen Y Z and Wu B 2005 *Chin. J. Geophys.* **48** 807
[26] Zheng W, Lu X L, Xu H Z and Luo J 2005 *Prog. Nat. Sci.* **15** 596
[27] Cheng L Y and Xu H Z 2006 *Chin. J. Geophys.* **49** 93
[28] Zheng W, Shao C G, Luo J and Xu H Z 2006 *Chin. J. Geophys.* **49** 644
[29] Zhou X H, Xu H Z, Wu B, Peng B B and Lu Y 2006 *Chin. J. Geophys.* **49** 718
[30] Zheng W, Shao C G, Luo J and Xu H Z 2008 *Prog. Nat. Sci.* **18** 555
[31] Zheng W, Xu H Z, Zhong M, Yun M J, Zhou X H and Peng B B 2008 *Chin. J. Geophys.* **51** 1143
[32] Zheng W, Xu H Z, Zhong M and Yun M J 2008 *Chin. Phys. Lett.* **25** 4482
[33] Zheng W, Xu H Z, Zhong M and Yun M J 2009 *Chin. Phys. Lett.* **26** 029101
[34] Zheng W, Xu H Z, Zhong M and Yun M J 2009 *Chin. Phys. B* **18** 3597
[35] Zheng W, Xu H Z, Zhong M, Yun M J, Zhou X H and Peng B B 2009 *Chin. J. Geophys.* **52** 564
[36] Zheng W, Xu H Z, Zhong M, Yun M J, Zhou X H and Peng B B 2009 *Chin. J. Geophys.* **52** 772
[37] Zheng W, Xu H Z, Zhong M, Yun M J, Zhou X H and Peng B B 2009 *Chin. J. Geophys.* **52** 1200
[38] Zheng W, Xu H Z, Zhong M, Yun M J, Zhou X H and Peng B B 2010 *Chin. J. Geophys.* **53** 218
[39] Zheng W, Xu H Z, Zhong M, Yun M J, Zhou X H and Peng B B 2010 *Chin. Astron. Astr.* **34** 413
[40] Zheng W, Xu H Z, Zhong M and Yun M J 2011 *Trans. Jpn. Soc. Aero. Space Sci.* **54** 106
[41] Zheng W, Xu H Z, Zhong M and Yun M J 2011 *J. Astronaut.* **32** 697
[42] Zheng W, Xu H Z, Zhong M and Yun M J 2012 *IEEE Geosci. Remote S.* **9** 422
[43] Zheng W, Xu H Z, Zhong M and Yun M J 2012 *Chin. J. Geophys.* **55** 1334